European Journal of Medicinal Chemistry 47 (2012) 24–37

Contents lists available at SciVerse ScienceDirect

European Journal of Medicinal Chemistry

journal homepage: http://www.elsevier.com/locate/ejmech

Original article

Molecular mechanism of serotonin transporter inhibition elucidated by a new flexible docking protocol

Mari Gabrielsen [a], Rafał Kurczab [b], Aina W. Ravna [a], Irina Kufareva [c], Ruben Abagyan [c], Zdzisław Chilmonczyk [d], Andrzej J. Bojarski [b], Ingebrigt Sylte [a,*]

[a] Medical Pharmacology and Toxicology, Department of Medical Biology, Faculty of Health Sciences, University of Tromsø, N-9037 Tromsø, Norway
[b] Department of Medicinal Chemistry, Institute of Pharmacology, Polish Academy of Sciences, 12 Smętna Street, 31-343 Kraków, Poland
[c] Skaggs School of Pharmacy and Pharmaceutical Sciences, 9500 Gilman Drive, MC 0747 La Jolla, California 92093-0747, United States
[d] National Medicines Institute, 30/34 Chełmska Street, 00-725 Warsaw, Poland

ARTICLE INFO

Article history:
Received 11 April 2011
Received in revised form
16 August 2011
Accepted 30 September 2011
Available online 20 October 2011

Keywords:
SERT homology models
SERT inhibitors
4D flexible docking
Structure-based pharmacophore models
Virtual screening
ICM

ABSTRACT

The two main groups of antidepressant drugs, the tricyclic antidepressants (TCAs) and the selective serotonin reuptake inhibitors (SSRIs), as well as several other compounds, act by inhibiting the serotonin transporter (SERT). However, the binding mode and molecular mechanism of inhibition in SERT are not fully understood. In this study, five classes of SERT inhibitors were docked into an outward-facing SERT homology model using a new 4D ensemble docking protocol. Unlike other docking protocols, where protein flexibility is not considered or is highly dependent on the ligand structure, flexibility was here obtained by side chain sampling of the amino acids of the binding pocket using biased probability Monte Carlo (BPMC) prior to docking. This resulted in the generation of multiple binding pocket conformations that the ligands were docked into.

The docking results showed that the inhibitors were stacked between the aromatic amino acids of the extracellular gate (Y176, F335) presumably preventing its closure. The inhibitors interacted with amino acids in both the putative substrate binding site and more extracellular regions of the protein. A general structure–docking-based pharmacophore model was generated to explain binding of all studied classes of SERT inhibitors. Docking of a test set of actives and decoys furthermore showed that the outward-facing ensemble SERT homology model consistently and selectively scored the majority of active compounds above decoys, which indicates its usefulness in virtual screening.

1. Introduction

The serotonin (5-hydroxytryptamine (5-HT)) transporter (SERT) is located in the membrane of presynaptic serotonergic neurons and transports the neurotransmitter 5-HT back into the presynaptic neuron after its release into the synaptic cleft. After its reuptake, 5-HT is either deaminated (i.e., inactivated) by the monoamine oxidase (MAO) enzyme or recycled into storage vesicles [1]. Hence, SERT plays an important role in termination of 5-HT mediated neuronal signalling. SERT belongs to the large neurotransmitter:sodium symporter (NSS) family of transporters [2] and is closely related to the dopamine and noradrenalin (norepinephrine) transporters (DAT and NET, respectively) [3]. The transporter is a target for approved therapeutics as well as several illicit drugs: the two main groups of antidepressant drugs, the tricyclic antidepressants (TCAs) and the selective serotonin reuptake inhibitors (SSRIs), act on SERT, as do psychostimulant compounds such as amphetamines and cocaine [4].

SERT contains 630 amino acids that are predicted to form 12 transmembrane α-helices (TMs) connected by intra- and extracellular loops (ILs and ELs, respectively). The 3-dimensional (3D) structure of SERT or of any other eukaryotic NSS homologue is not known, however, several 3D structures of a bacterial homologous transporter, the *Aquifex aeolicus* leucine transporter (LeuT), are available [5–9]. Interestingly, LeuT has been cocrystallised with SERT inhibitors belonging to the TCA (clomipramine, imipramine and desipramine) and SSRI (sertraline and (*R*)- and (*S*)-fluoxetine) classes of antidepressant drugs [6,8,9]. In these crystal structures, they are found to bind as (low-affinity) non-competitive inhibitors

Abbreviations: *5-HT*, 5-hydroxytryptamine; *SERT*, serotonin transporter; *DAT*, dopamine transporter; *NET*, noradrenaline (norepinephrine) transporter; *SSRIs*, selective serotonin reuptake inhibitors; *TCAs*, tricyclic antidepressants; *PI*, positive ionisable feature; *AR*, aromatic feature; *HYD*, hydrophobic feature; *HBA*, hydrogen bond acceptor feature.

* Corresponding author. Tel.: +47 77644705; fax: +47 77645310.
E-mail address: ingebrigt.sylte@uit.no (I. Sylte).

0223-5234/$ – see front matter © 2011 Elsevier Masson SAS. All rights reserved.
doi:10.1016/j.ejmech.2011.09.056

in a second binding site (hereafter: the vestibular binding site) that is situated approximately 11 Å above the substrate binding site and are separated from the substrate binding site by the side chains of the two aromatic amino acids of the extracellular gate. The localisation of the vestibular site as the primary TCA- and SSRI- binding site in SERT is, however, controversial as several experimental studies on SERT suggest that these inhibitors act in a competitive manner by binding to the substrate binding site [10–13]. In contrast to the crystal structures of LeuT cocrystallised with TCAs and SSRIs, the 3D structure of LeuT and L-tryptophan shows that this compound is a competitive inhibitor that locks LeuT in an outward-facing conformation [5]. The binding site in this conformation consists of regions belonging to the substrate binding site and of more extracellular regions of the transporter [5]. SERT inhibitors are thought to stabilise more outward-facing conformations of SERT [14,15], the only exception being ibogaine which has been proposed to stabilise SERT in an inward-facing conformation [16]. Thus, the binding pocket detected in a homology model of SERT based on the crystal structure of LeuT in an outward-facing conformation may represent a realistic pocket for docking of inhibitors in SERT and contribute to increased understanding of SERT inhibition.

As early as in 1966, transporter proteins were proposed to transport substrates through an alternate-access mechanism, where a centrally located substrate binding site alternately is exposed to either the extracellular environment (outward-facing conformation) or the cytoplasm (inward-facing conformation), achieved by significant conformational changes of the proteins [17]. Hence, the LeuT crystal structures, in which the LeuT structure are in either intermediate occluded conformation or in an outward-facing conformation, are in agreement with this proposed transport mechanism, though no crystal structure of the inward-facing LeuT protein has been determined. However, the detailed transport mechanism of NSS family members is still unknown, though it is clear that in order for transport to occur large protein rearrangements must take place. Inclusion of SERT flexibility during docking may also be crucial as the SERT homology models based on the crystal structures of LeuT most likely are not in the totally correct SERT inhibitor binding conformations as the sequence identity between LeuT and SERT is low.

In this study a new flexible docking protocol was applied in order to take into account SERT binding pocket flexibility. The protocol consists of (1) detection of the ligand binding pocket using ICM PocketFinder [18], (2) side chain sampling of the amino acids detected during the previous step using biased probability Monte Carlo (BPMC) implemented in ICM [19], and (3) 4D flexible docking and scoring of the ligands [20] (Fig. 1). The protocol was used to dock 58 known SERT inhibitors belonging to the SSRI-, TCA-, 3-phenyltropane derivative-, mazindol derivative- and radioligand-groups. The resulting inhibitor binding modes have also been combined in a general structure–docking-based pharmacophore model constructed based on the spatial distribution of the pharmacophore features in structure–docking-based models of the four most populated SERT binding pocket conformations. The general pharmacophore model covered all classes of SERT inhibitors studied. Our results suggest that inhibitors contact amino acids belonging to both the putative substrate binding site and the vestibular binding site, and that they may inhibit transport in SERT by preventing the extracellular gate from closing. Furthermore, docking of a test set containing 19 actives and 190 decoys also suggested that the obtained model ensemble was capable of discriminating actives from decoys and that the models may therefore be a valuable tool for target-based virtual screening.

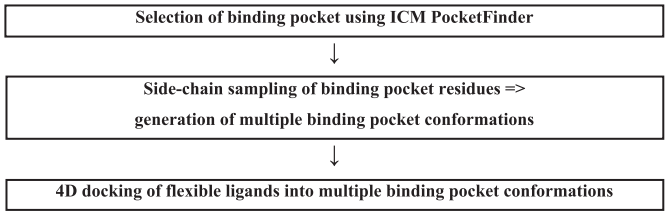

Fig. 1. Schematic overview over the flexible docking protocol.

2. Experimental

2.1. SERT homology modelling

Two SERT (UniProtKB/Swiss-Prot [21] accession number P31645) homology models were constructed based on a comprehensive alignment of prokaryotic and eukaryotic NSS transporter sequences [3]. The crystal structure of the outward-facing conformation of LeuT cocrystallised with L-tryptophan (PDB id 3F3A) [5] was used as a template for one of the models (outward-facing model), while the x-ray structure of LeuT cocrystallised with imipramine (PDB id 2Q72) [6] was used a template for the second model (occluded model).

The overall sequence identity between LeuT and SERT is approximately 21 percent but rises to 35 percent in the TMs involved in substrate binding (TMS 1, 3, 6 and 8) [3]. The loops are the regions of lowest homology between the two transporters [3]. ICM [22] version 3.5 BuildModel macro was used for construction of the homology model. The macro constructs the conserved transmembrane helices using core sections defined by the average of C_α atom positions in these regions and performs a PDB database loop search by matching the loop regions in regard to sequence similarity and steric interactions with the surroundings of the model.

2.2. Energy refinement and regularisation

Following homology modelling, energy refinement of the SERT models were performed using the refineModel macro of ICM [22]. The macro performs side chain conformational sampling, followed by 5 steps of iterative annealing of the backbone and a second side chain sampling to resolve any problems that may have resulted from the threading step. The side chain optimisation steps were performed by the program module Montecarlo-fast [19] included in the refineModel macro. Iterations of this rapid side chain optimisation procedure consist of random move followed by local energy minimisation of a subset of the side chains of SERT residues, which accelerates the calculation as opposed to minimising all SERT side chains. The side chain subset that is minimised is established based on the energy-gradient generated during the random move and only the side chains above the energy-gradient threshold are minimised. These side chains usually belong to the residues that are not conserved between the template and target structures and to a certain degree also their conserved neighbouring residues. Each Montecarlo-fast iteration is either accepted or rejected based on the energy and temperature. The backbone annealing step of the refinement is performed with tethers, which are harmonic restraints that pull on each atom in SERT to a static point in space represented by a corresponding atom in the template.

The energy refined SERT homology models were also regularised, or fitted with the ideal covalent geometry of residues. The regularisation procedure of ICM generates an extended all-atom model of the protein with regular geometry characteristics and assigns the non-hydrogen atoms in the model to the equivalent atoms in the model before it builds the regularised structure. It then

rotates methyl groups to reduce van der Waals del clashes and optimises the combined geometry and energy function before the polar hydrogen positions are adjusted.

2.3. Structure quality check

The structural quality of the refined/regularised SERT homology models was checked by uploading the models to http://nihserver.mbi.ucla.edu/SAVES_3/. The outward-facing model was found satisfactory with an ERRAT quality factor of 88.996 and the Ramachandran plot provided by ProCheck showed that 91.8 percent of the residues were in the core regions. The structure of the occluded model was similarly satisfactory with an ERRAT quality factor of 82.819 and 89.4 percent of the amino acids in the core regions as shown by the Ramachandran plot. WhatCheck was also satisfactory for both models.

2.4. SERT inhibitors

The inhibitors were constructed in their protonated state using the ICM ligand editor. Ligands from five different chemical groups were included in the study, namely SSRIs ((*S*)-citalopram, desmethyl-(*S*)-citalopram, didesmethyl-(*S*)-citalopram, (*S*)-LU-08-052-O, (*S*)-LU-33-086-O, (*RS*)-fluoxetine, desmethyl-(*RS*)-fluoxetine, (*RS*)-venlafaxine, O-desmethyl-(*RS*)-venlafaxine, fluvoxamine, sertraline, and desmethyl-sertraline), TCAs (amitriptyline, clomipramine, desipramine, imipramine, protriptyline and (*RS*)-trimipramine), 3-phenyltropanes (cocaine, AB-248, AB-338, β-CFT, CPT-D-tartrate, RTI-31, RTI-32, RTI-55 (β-CIT), RTI-83, RTI-112, RTI-121, RTI-142, RTI-311 and SN-1), mazindol derivatives ((*RS*)-mazindol, (*RS*)-mazindane, (*RS*)-MAZ-10, (*RS*)-MAZ-85, and (*RS*)-MAZ-89) and SERT radioligands (403U76, 4-FADAM, ADAM, AFM, DAPA, DASB, IDAM, MADAM, and ODAM). In total, 58 inhibitors were docked. In addition, protonation of the 3-phenyltropane and mazindol derivatives resulted in the generation of a chiral centre and both N^+ (*R*)- and (*S*)-forms of the compounds were thus docked. The (*S*)-forms of the compounds yielded the best docking results and were selected to represent these compounds in the paper.

2.5. Flexible docking protocol

2.5.1. Detection of the ligand binding pocket

The ICM PocketFinder algorithm (thoroughly described in reference [18]) was used to detect possible ligand binding pockets in the models. The algorithm uses a transformation of the Lennard–Jones potential calculated from a three-dimensional protein structure and does not require any knowledge about a potential ligand molecule, i.e. it is based solely on protein structure [18].

2.5.2. Fumigation

During this step, torsional sampling of the protein side chains took place in the presence of a repulsive density representing a *generic* ligand. To calculate this repulsive density, all the side chains of the amino acids in the selected pocket, except the side chains of alanine, glycine and cysteine amino acids, were simultaneously converted to alanine and an atom density grid map was generated for this "shaved" protein. Then, repeated spatial averaging of the map was performed to obtain a smoothed density map which fills the cavities of the original protein and the difference between the smoothed and the original maps was calculated. The internal variables that control the shape of the pocket are sampled using the biased probability Monte Carlo (BPMC) [19] sampling procedure implemented in ICM [22], with the generated density included as a penalty term in the combined energy function [23]. The BPMC procedure consists of (1) a random conformational change of the side chain torsion angles based on predefined probability distributions, followed by (2) local energy minimisation in side chain torsion angle space. The complete energy is calculated and the total energy is accepted or rejected before the procedure returns to (1) [19]. The resulting binding pocket conformations that were generated during fumigation were indexed according to their total energy. The user of the protocol can at this stage of the protocol select which binding pocket conformations to include in the docking step simply by deleting unwanted binding pocket conformations from the index.

2.5.3. Grid map generation

3D grid maps that represent the van der Waals, electrostatics, hydrophobic and hydrogen bonding potentials of the selected binding pocket residues were calculated using a grid spacing of 0.5 Å and a margin of 4 Å (default values), as during a regular rigid protein-flexible ligand docking. 3D grids are then generated sequentially for the binding pocket conformations available in the index. The 3D grids of each conformation are stored as a single data structure, referred to as the 4D grid. Hence, in the 4D grid, the first three dimensions represent regular Cartesian coordinates of the grid sampling nodes, whereas the fourth dimension represents an index of the pocket conformations.

2.5.4. Ligand sampling (docking) and scoring

A set of ligand conformers were generated by ligand sampling *in vacuo*, placed into the binding pocket in four principal orientations and used as starting points for Monte Carlo global energy optimisation [23]. During Monte Carlo sampling, the ligand is allowed to change the fourth coordinate via a special type of random move alongside the regular Cartesian translations and rotations [23]. Finally, the ICM VLS (virtual ligand screening) scoring function is used to score the ligand binding modes. The VLS scoring function uses steric, entropic, hydrogen bonding, hydrophobic and electrostatic terms to calculate the score and also includes a correction term proportional to the number of atoms in the ligand to avoid bias towards larger ligands [24].

2.5.4.1. Docking to the outward-facing SERT model. An ICM PocketFinder [18] tolerance level of 3 was used to detect the ligand binding pocket in the outward-facing SERT conformation. The following SERT amino acid side chains were detected as being part of the binding pocket and selected for side chain sampling using BPMC in step 2: Y95, D98, L99, W103, R104 and Y107 in TM1; I172, Y175, Y176 and I179 in TM2; F335, S336, L337, F341 and V343 in TM6; K399, D400, P403, L405, L406 and F407 in EL4; S438 and T439 in TM8; and E493 and T497 in TM10. The fumigation resulted in 47 low energy SERT binding pocket conformations, all of which were included in the 4D grid map. Three parallel docking simulations of the ligands in the five classes of SERT inhibitors were performed. The best binding mode of each ligand was selected from the three parallel dockings based on the following criteria: first, only ligand binding modes where the protonated amine moiety of the ligands may interact with the negatively charged D98 in TM1 were accepted. For each ligand, the best energy conformation of the accepted ligands was then selected as the best binding mode. Only the top-scored pose of each inhibitor was evaluated.

2.5.4.2. Docking to the occluded SERT homology model. In order to define the vestibular SERT-ligand binding pocket in the occluded model, the occluded SERT model and the LeuT template were superimposed and imipramine copied from the LeuT crystal structure into the SERT model. The following amino acids were sampled during the fumigation step of the flexible docking protocol: L99, W103, R104, Y107, I108, Y175, Y176, F335, K399,

D400, P403, K490, and E493. The 58 inhibitors were docked into 10 binding pocket conformations using the 4D docking approach. Three parallel docking runs were performed.

2.6. Structure–docking-based pharmacophore model generation

Structure–docking-based pharmacophore models of the most populated SERT binding pocket conformations (conformations 18, 23, 24 and 32) of the outward-facing SERT model were generated using tools and protocols implemented in the Discovery Studio package version 2.5 [25]. Inhibitors from all classes of the docked SERT inhibitors were found to bind in these binding pocket conformations. The docking poses of RTI-31, RTI-55 (β-CIT), RTI-121 (3-phenyltropane derivatives), ODAM, ADAM (radioligands), and (*S*,*S*)-MAZ-85 (mazindol derivatives) were used for generation of the structure–docking-based pharmacophore model of binding pocket conformation 18 and (*S*)-LU-08-052-O (SSRI), imipramine, (*R*)-trimipramine, (*S*)-trimipramine (TCAs), β-CFT, RTI-311 (3-phenyltropanes), 403U76, DASB, IDAM, MADAM (radioligands) were used to generate the structure–docking-based pharmacophore model of binding pocket conformation 23. For binding pocket conformation 24 and 32, the docking poses of didesmethyl-(*S*)-citalopram, O-desmethyl-(*S*)-venlafaxine (SSRIs), amitriptyline, clomipramine, desipramine (TCAs), (*R*)-MAZ-10 (mazindol derivatives) and DAPA (radioligand) (conformation 24) and the docking poses of AB-338 (3-phenyltropane derivative), AFM (radioligand), (*R*)-mazindol, (*S*)-mazindane and (*R*)-MAZ-89 (conformation 32) were used to generate the structure–docking-based pharmacophore models.

The standard procedure for generation of a ligand-based pharmacophore model was modified in order to generate the structure–docking-based pharmacophore models. The pharmacophore models were generated using the exact geometry of the ligands from the 4D docking procedure. The docked ligand conformations were mapped to a set of pharmacophore features, namely hydrogen bonding acceptor (HBA), positive ionisable group (PI), the hydrophobic region (HYD) and the aromatic ring (AR). Within the given SERT conformation, a comprehensive map of the spatial distribution of various pharmacophore points in the binding site cavity was obtained. Clustering of the same type of pharmacophore features was then performed, taking into account the calculated distances between all possible pairs of feature centroids as a classification criterion. On the basis of the obtained dendrograms, which show the cluster distribution of individual pharmacophore features, the densest clusters were selected, for which the average position for a given feature was calculated. In addition, the correctness of the feature cluster choice was examined by visual inspection of its distribution in SERT. A cluster representing a given pharmacophore feature was accepted if it was located near the amino acid or group of amino acid side chains responsible for a given type of interaction with the ligand. In this way, the obtained model was based on conformations of known ligands docked into a set of different SERT conformations and an analysis of their interactions with amino acids side chains in the binding site was averaged by the spatial distribution of pharmacophore features. To compare the complementarity and similarity of the created structure–docking-based pharmacophore models, a rigid alignment without the optimisation of pharmacophore features position, was generated. The Pharmacophore Comparison procedure from the Pharmacophore Protocol in Discovery Studio [25] was used to calculate the RMSD between the all four models in the alignment.

2.7. Evaluation dockings

A test set containing 19 compounds with known SERT activity and 190 decoys (supporting information) was used to evaluate the generated models, thus obtaining a 1:10 ratio between actives and decoys. The 19 active compounds (defined as compounds with SERT Ki $<$ 50 nM) and 13 inactive compounds (defined as compounds with SERT Ki $>$ 10 000 nM) were selected from the ChEMBL database. In order to reach a 1:10 active to inactive ratio, a set of 44 and 133 topologically dissimilar compounds to the active compounds were selected as decoys from the ChemDiv and ChemBridge databases, respectively. Only non-chiral compounds or compounds with definite chirality were included in the test set. Clustering of the decoys using the TREE method with UPGMA (unweighted pair group method using averages) linkage type available in ICM [22] also showed that they were diverse in structures. The decoys resembled the physical properties of the active compounds such that enrichment was not simply a separation of trivial physical features. The compounds selected from ChemDiv and ChemBridge had Tanimoto coefficients below 0.5, they contained one or more protonated amine moieties and their average molecular weight (MW) was 333.41 Da as compared with an average MW of 316.47 Da for the actives.

The evaluation test set was docked using the 4D docking protocol [20] into 47 binding pocket conformations of the outward-facing homology model. Three parallel dockings were performed. The test set was also docked once into the binding pocket detected using an ICM PocketFinder [18] tolerance level of 3 in the outward-facing SERT homology model using a regular rigid receptor–flexible ligand docking protocol.

For the evaluation of the classification performance, several indices (enrichment factor (EF), Matthews correlation coefficient (MCC) [26], accuracy, precision and recall (sensitivity)) were calculated using scoring values <0 and score <-10 as thresholds. At score threshold <0, true positives (TP) were defined as actives that interacted with D98, false positives (FP) were decoys that interacted with D98, true negatives (TN) were decoys that either had positive scores or did not interact with D98 and false negatives (FN) were actives that either had positive scores or did not interact with D98. At score threshold <-10, the actives that had scores higher than -10 were also selected as false negatives and decoys as true negatives.

Enrichment factor (EF) is the most used measure to evaluate a docking screen. The factor describes the capability of the docking program to enrich the small number of known actives in the top ranks of a screen among a much higher number of decoys in the database [27]:

$$EF = (HITS_{sampled}/N_{sampled})/(HITS_{total}/N_{total}); \text{ or } ((TP/(TP + FP))/((TP + FN)/(TP + FN + TN + FP))$$

The higher percentage of known ligands found at a given percentage of the top ranked database, the better the enrichment performance of the docking screen. A complementary measure of the prediction accuracy is the Matthews correlation coefficient (MCC) [26], used to reflect the correlation between the predicted and the observed result:

$$MCC = ((TP\times TN) - (FP\times FN))/((TN + FP)\times(TN + FN)\times(TP + FP)\times(TP + FN))\ \hat{}\ 0.5$$

The MCC values range from -1 to 1, a perfect prediction having a MCC of 1. The accuracy, precision and recall parameters should be seen together as they are not absolute indicators of classification performance by themselves. They were defined by:

$$Accuracy = (TP + TN)/(TP + FP + TN + FN)$$

$$Precision = TP/(TP + FP)$$

Recall (sensitivity) = TP/(TP + FN)

Accuracy is the overall classification accuracy of the model including both the active and inactive compounds, whereas precision is a measure of the capability of predicting active compounds. Recall (sensitivity) is the percentage of truly active compounds being selected.

The flexible docking protocol was also tested in a cross-docking study using experimentally determined 3D structures. Two protein–ligand crystal structure complexes of LeuT (PDB id 2A65 and 3F3C), cyclooxygenase-2 (COX-2; PDB id 3PGH and 1CX2) and of the oestrogen receptor (PDB id 1ERR and 3ERT) were used in the cross-docking study, docking the ligand from one complex into the receptor of the other complex and vice versa. The following LeuT amino acids were selected for side chain sampling: N21, L25, N27, V104, Y108, F253, T254, S256, F259 and I359. The following COX-2 amino acids were selected for side chain sampling: H90, T94, V116, R120, Q192, Y348, Y335, V349, L352, S353, L359, L384, F381, Y385, W387, R513, P514, D515, I517, F518, M522, V523, S530 and L531. The following oestrogen receptor amino acids were selected for side chain sampling: M343, L346, T347, L349, D351, E353, L354, W383, L384, L387, M388, L391, R394, F404, E419, M421, I424, L428, H524, L525 and L536. Only the top-scored conformation of each ligand was evaluated. The heavy atom root mean square deviation (RMSD) between the ligand in docked complex and in the experimentally determined complex was then calculated. A similar cross-docking study was also performed using a regular semi-flexible docking approach.

2.8. Refinement

Based on the docking results obtained during the flexible docking of the 58 known inhibitors into the outward-facing SERT homology model, five SERT-ligand complexes (SERT-403U76 (conformation 23), SERT-didesmethyl-(*S*)-citalopram (conformation 24), SERT-imipramine (conformation 18), SERT-(*R*)-mazindol (conformation 32) and SERT-RTI-311 (conformation 18)) were refined. 5 refinements of each SERT-ligand complex were performed. First, local refinement of the initial docking complexes was performed with the ligands tethered to their docked conformations. Next, flexible side chain docking was performed with global sampling of both the ligand and the pocket. During this simulation, a distance restraint between D98 in the transporter and the basic ligand centre was imposed. Local refinements of the flexible docking results were also performed. Next, the alignment between LeuT and SERT in EL4 was slightly adjusted with respect to the comprehensive alignment published [3]. Flexible docking and local refinement of the flexible docking results in the adjusted models were then performed. Finally, the evaluation test set compounds were docked into the 25 refined models and the enrichment factors were calculated.

3. Results

3.1. Homology modelling and flexible docking

3.1.1. Outward-facing homology model

A SERT homology model, based on the LeuT crystal structure cocrystallised with the competitive inhibitor L-tryptophan [5], was constructed using ICM [22] (Fig. 2) and used for docking. As the L-tryptophan inhibitor caused LeuT to stabilise in an outward-facing conformation, the binding pocket detected by ICM PocketFinder [18] in the SERT homology model based on this crystal structure was larger than in the occluded conformation of the transporter published previously [28]. In the occluded state, the side chains of the amino acids constituting the extracellular gate (Y176, F335)

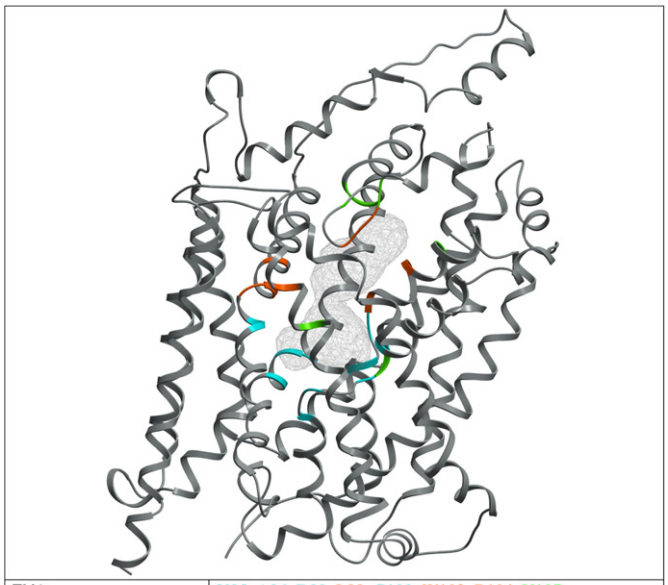

Fig. 2. C_α-backbone trace of the outward-facing homology model of SERT seen in membrane plane. The binding pocket detected by ICM PocketFinder is shown as grey wire, with the C_α-backbone of the amino acids of the pocket (colour coding in accordance to table). Blue amino acids: part of substrate binding site in the occluded SERT conformation; orange amino acids: part of the vestibular binding site in the occluded SERT conformation; green amino acids: not detected as part of the substrate binding site or the vestibular binding site in the occluded SERT conformation.

blocked the access to the putative substrate binding site from the extracellular environment and hence, two binding pockets, namely the substrate binding pocket and the vestibular binding pocket, were detected. These binding pockets were located below and above the extracellular gate, respectively (Fig. 2). The binding pocket detected in the outward-facing model had an inverted Y-shape, with the V-part of the letter representing the putative substrate binding site described experimentally [10–13] and the I-part representing a vestibule that extended from the putative substrate binding site towards the extracellular environment (Fig. 3). Amino acids from TM1, TM3, TM6 and TM8, as well as from EL4 and TM10, lined the pocket in the outward-facing model (Fig. 3). TMs 1 and 6 were partly unwound (A96-D98 and L337-G342, respectively, as in the occluded conformation of SERT), and amino acids Y175 in TM2 and S438 in TM8 were also located in partly unwound regions (Fig. 3). The amino acids detected as being part of the binding pocket are mainly hydrophobic in character, though some charged amino acids line the vestibule part of the pocket (Fig. 3).

A new flexible docking procedure (Fig. 1) was used to dock the 58 inhibitors into the outward-facing model of SERT. Using this procedure, multiple conformations of the outward-facing binding pocket were generated through side chain sampling of the amino acids lining the pocket using biased probability Monte Carlo (BPMC) [19] implemented in ICM [22]. The side chain sampling resulted in 47 energetically favourable binding pocket conformations that then were treated together in a single docking run (4D docking [20]). Known SERT inhibitors are very diverse in structure and most likely bind to different SERT conformations [14,29]. Thus, including multiple pocket conformations may improve the docking results as the chances of an inhibitor recognising a suitable

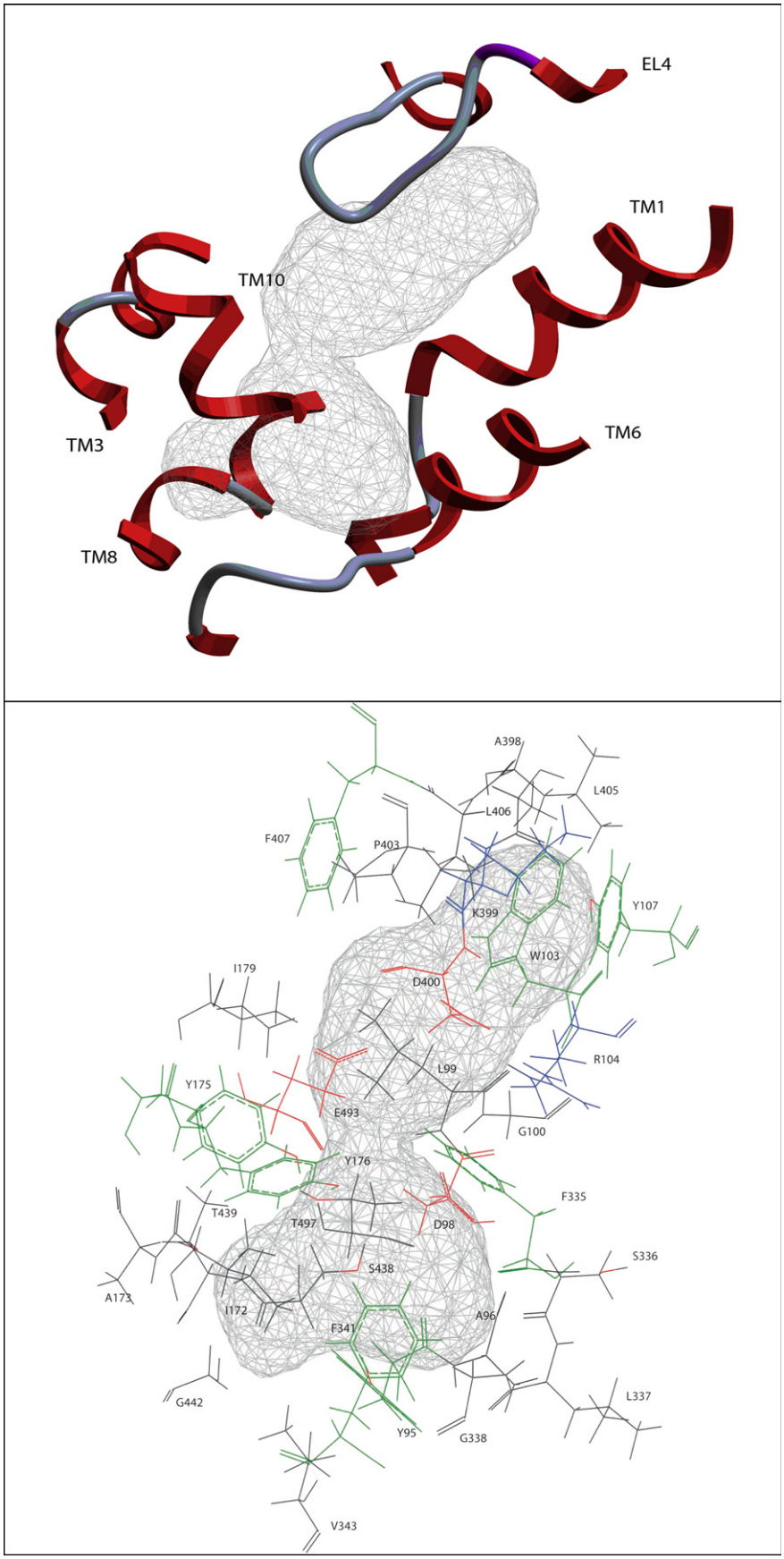

Fig. 3. Binding pocket detected by ICM PocketFinder in the outward-facing conformation of SERT. Upper: amino acids 94–110 (TM1), 172–179 (TM3), 330–343 (TM6), 395–407 (EL4), 435–442 (TM8) and 492–498 (TM10) are shown as ribbon (red/grey). Lower: amino acid coloured according to their properties. Hydrophobic amino acids are shown as grey wire representation, aromatic amino acids as green wire, negatively charged amino acids as red wire and positively charged amino acids as blue wire. For clarity the hydroxyl oxygen atoms of tyrosine, serine and threonine amino acids have been coloured red.

conformation for binding increase. Also, as SERT inhibitors are larger compounds than L-tryptophan, the distance between Y176 and F335 most likely ought to be increased even more to accommodate the SERT inhibitors. Indeed, our docking results (Fig. 5, supporting information) show that the most occupied SERT binding pocket conformations (containing more than 50 percent of the docked compounds) were conformations 18, 23, 24 and 32 (Fig. 4), all of which had a distance between Y176 and F335 larger than in the initial outward-facing SERT homology model (Fig. 4). The side chain of F335 was the more flexible of the two; in conformations 18, 23 and 32 this side chain had flipped approximately 90° as compared with the occluded SERT conformation (Fig. 4).

Three parallel dockings of the inhibitors into the 47 binding pocket conformations were performed using the 4D docking protocol [20]. The top-scored binding mode of each ligand that had its protonated amine moiety in the vicinity of D98 was selected to represent the inhibitor (Fig. 5, supporting information). The possible ionic interaction with this aspartic acid, located in the putative substrate binding site of SERT, was the most important criterion when selecting the inhibitor binding modes as this amino acid is assumed to be the anchoring point of both substrates and inhibitors in SERT [11,30–33]. Indeed, the docking results showed that the majority of the ligands may interact with the D98: of the 58 ligands docked, only four inhibitors (AB-248, RTI-142, (*S*)-mazindol and (*S*)-venlafaxine) did not have their protonated amine group near D98 as the top-scored binding mode in any of the three parallel dockings that were performed. The results showed that the inhibitors occupied parts of the putative substrate binding pocket but also protruded into the vestibule extending towards the extracellular environment (Fig. 5). In addition to the D98 interaction, many inhibitors had an aromatic moiety juxtaposed between the aromatic amino acids of the extracellular gate, Y176 and F335, and hydrophobic or aromatic moieties in the vicinity of A169, I172, A173 and V343.

3.1.2. Occluded homology model

The TCAs imipramine, desipramine and clomipramine and the SSRIs sertraline and (*RS*)-fluoxetine have been cocrystallised with LeuT [6,8,9]. The crystal structures show that the inhibitors, which are low-affinity LeuT inhibitors, interact in the vestibular region and stabilise an occluded conformation of the transporter. Flexible docking into the vestibular region in an occluded SERT homology model generated based on the LeuT-imipramine crystal structure (PDB id 2Q72) was hence performed. The docking results showed that the ligands in SERT occupied a region between TMs 1, 6 and 10 and EL4 that only partly corresponded to the region occupied by imipramine in LeuT (Fig. 7). The majority of the cocrystallised TCA and SSRI inhibitors interact with LeuT D401 [6,8,9], which corresponds to SERT K490. Our docking results suggest that D328 (TM6) or E493 and E494 (TM10) may contribute in the binding of the inhibitors in the vestibular binding pocket (Fig. 7). However, in comparison with the results obtained from docking of the ligands into the 47 conformations generated of the binding pocket detected in the outward-facing SERT homology model, the orientations of the inhibitors in the vestibular binding site varied significantly, even between the highly similar members of the same inhibitor classes (e.g. the TCAs and radioligands). No further work was hence performed using the occluded SERT model.

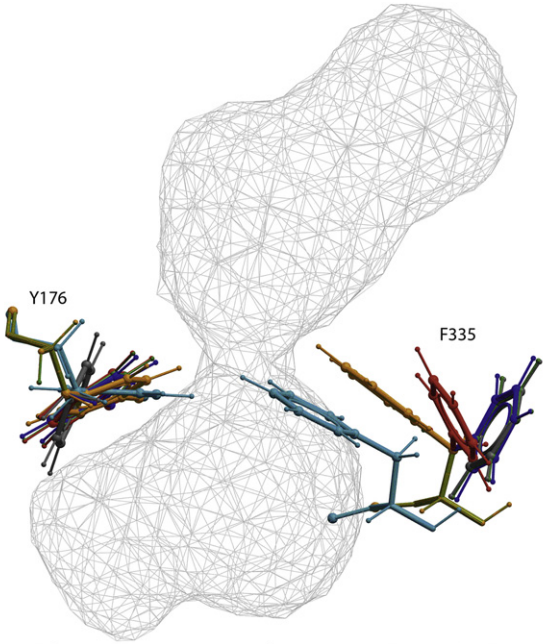

Shortest distance (Å) Y176-F335	SERT conformation
2.3	Occluded homology model
4.4	Outward-facing homology model
12.6	Binding pocket conformation 18
11.9	Binding pocket conformation 23
8.7	Binding pocket conformation 24
12.1	Binding pocket conformation 32

Fig. 4. Comparison of Y176 and F335 in the occluded conformation (cyan xstick representation), outward-facing conformation (orange xstick representation) and in binding pocket conformations 18, 23, 24 and 32 (green, grey, red and blue xstick representation, respectively) of SERT. The distances between Y176 and F335 (Å) are listed. The binding pocket detected in the outward-facing conformation of SERT is shown as grey wire.

3.2. Pharmacophore model generation

Hypothetical pharmacophore models based on the binding modes of the inhibitors binding in conformations 18, 23, 24 and 32 of the outward-facing SERT model were also generated to illustrate the docking results (Fig. 6). The pharmacophore models based on these four SERT structures were nearly identical. They contained the same number of features, namely one positive ionisable group

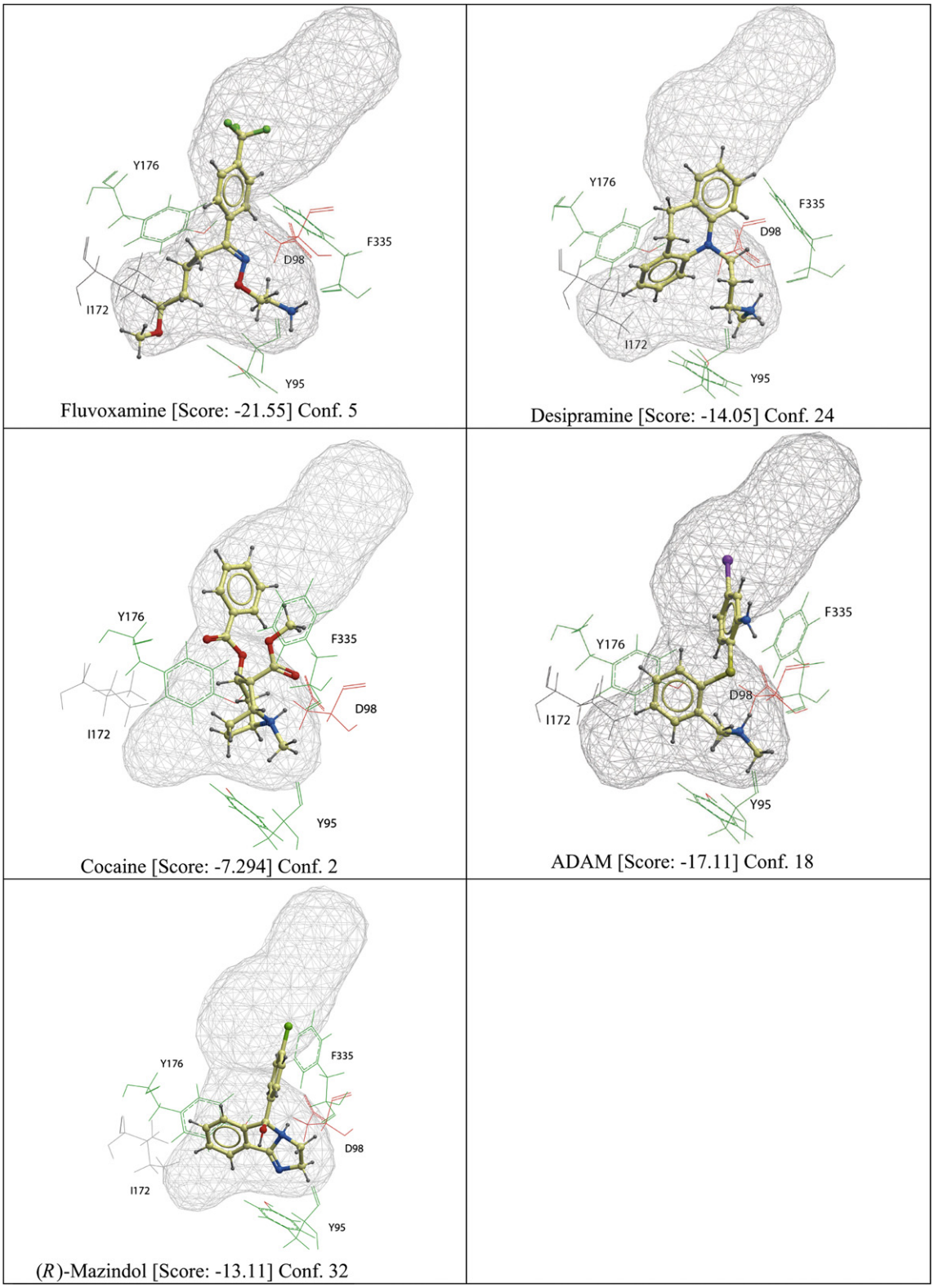

Fig. 5. Docking results. Fluvoxamine (SSRIs), desipramine (TCAs), cocaine (3-phenyltropane derivatives), ADAM (radioligands) and (*R*)-mazindol (mazindol derivatives) docked into the outward-facing SERT homology model using the 4D docking protocol. The binding pocket detected is represented as grey wire. The score is given in brackets and the SERT binding pocket conformation is also shown.

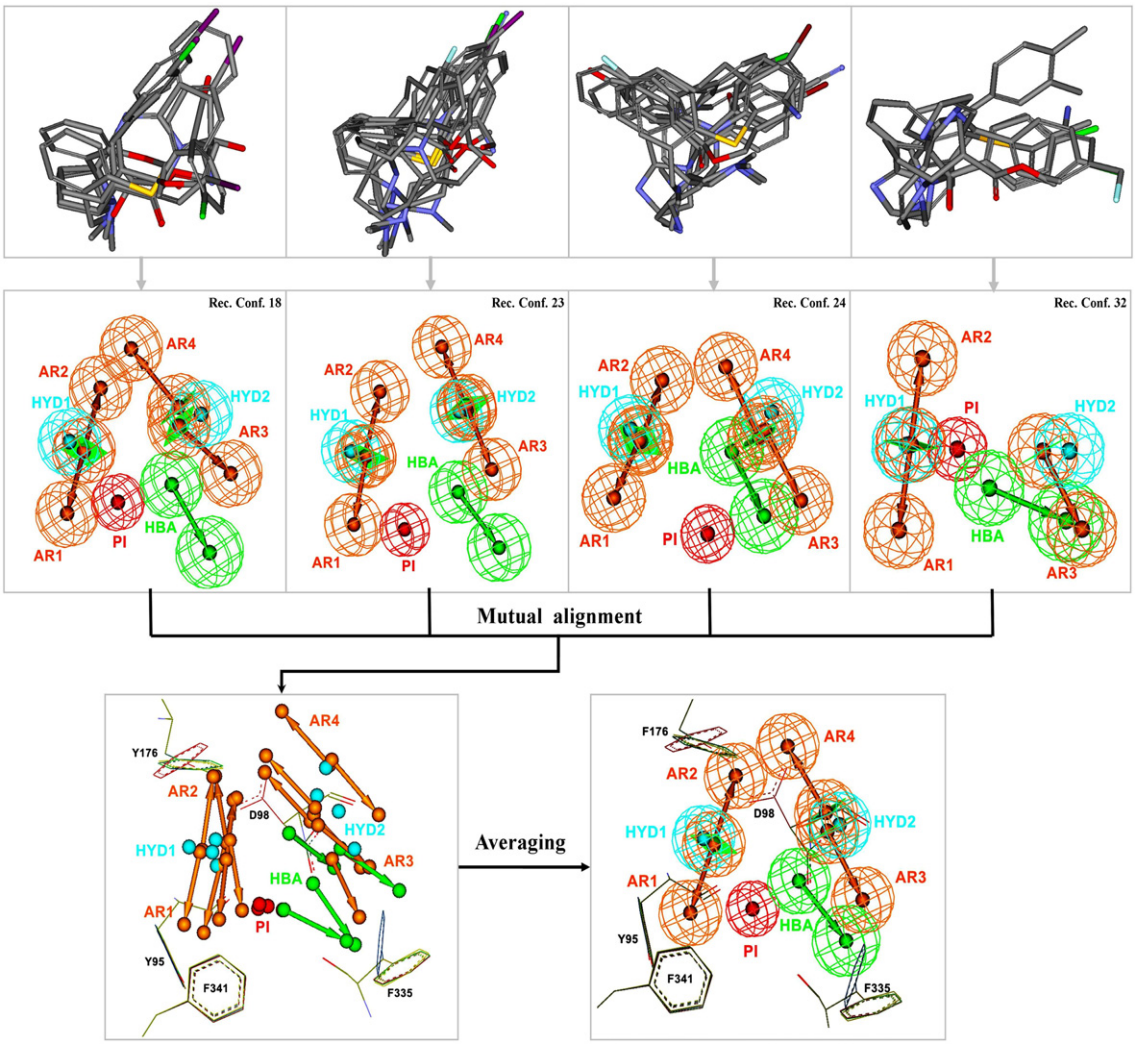

Fig. 6. Schematic representation of the generation of structure–docking-based pharmacophore models. No hydrogen atoms are shown. PI, positive ionisable feature; AR, aromatic feature; HYD, hydrophobic feature; HBA, hydrogen bond acceptor feature.

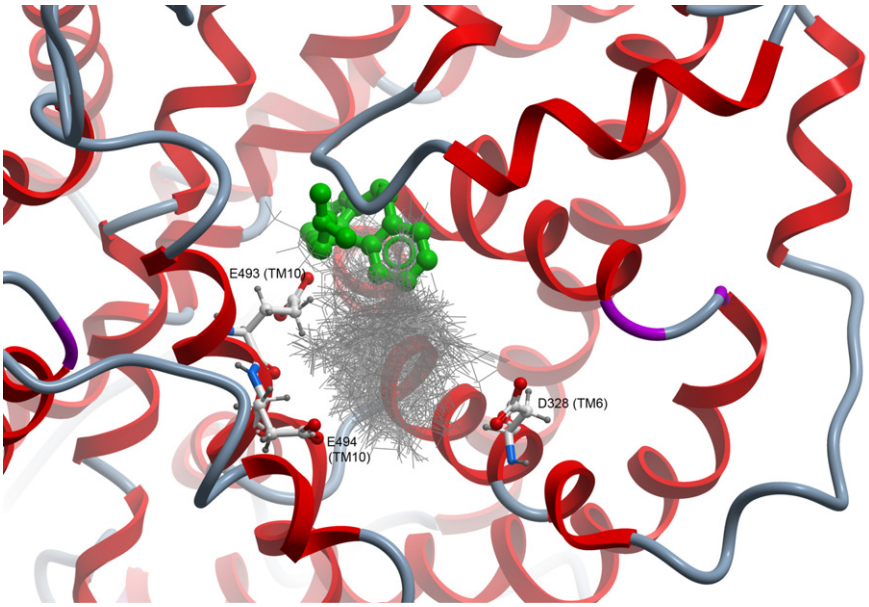

Fig. 7. Extracellular view of the 58 known SERT inhibitors (grey wire representation) docked into the vestibular binding pocket in the occluded SERT homology model based on the LeuT 2Q72 template. Imipramine (from the crystal structure) is shown in green xstick representation. Amino acids D328 (TM6), E493 and E494 (TM10) are also shown.

(PI) and one hydrogen bonding acceptor feature (HBA), as well as two hydrophobic (HYD) and four aromatic features (AR) (Fig. 6). The same pharmacophore features of the different models occupied the same areas in the binding site. The AR1 and AR2 features represented the interaction between aromatic ligand moieties and the side chains of Y176 and F341, and the positive ionisable group (PI) was in the vicinity of the negatively charged D98. The HBA and AR3 features pointed towards F335 (TM6); the HBA feature towards the backbone oxygen atom, and the AR3 feature towards the aromatic side chain of F335. The AR4 feature pointed in the direction of Y176 (Fig. 6). The HYD and AR features were overlapping, reflecting that not all inhibitors contained two aromatic rings but rather hydrophobic groups (Fig. 6). Mutual rigid alignment of the pharmacophore models also showed that the spatial distribution of the pharmacophore features was very consistent (Fig. 6), a fact further supported by the general pharmacophore model that was constructed based on the pharmacophore models of binding pocket conformations 18, 23, 24 and 32 (Fig. 6). Table 1 shows the results of the calculated RMSD values between the pharmacophore models and Table 2 shows the interfeature distances (Å) of the general pharmacophore model.

3.3. Evaluation of screening selectivity of the outward-facing model

The ability to separate active compounds from decoys of similar molecular weight and atomic composition is evidence of correct modelling of the key features of ligand–pocket interactions [34–37]. In order to evaluate whether our models could separate active from inactive compounds, a test set containing 19 actives and 190 decoys was assembled and docked into the 47 SERT binding pocket conformations previously generated using the 4D docking protocol [20]. The high-affinity SERT binders (SERT Ki $<$ 50 nM) in the test set were diverse in structure and were not among the 58 inhibitors already docked, whereas the decoys were a mixture of known inactive compounds (SERT Ki $>$ 10.000 nM) from the ChEMBL (https://www.ebi.ac.uk/chembldb) database and assumed inactive compounds selected from the ChemDiv (www.chemdiv.com) and ChemBridge (www.chembridge.com) databases. The decoys had physical properties within the range of the active compounds, however, differed structurally from the actives (supporting information).

The results from the three parallels of the evaluation docking are shown in Table 3. The test set docking results were analysed using two score thresholds, score <0 and score <-10. The accuracy values show that around 80 percent of the actives and decoys were correctly predicted at score threshold <0 and around 90 percent at score threshold <-10. As our test set contains ten times more decoys than actives, however, the accuracy is especially influenced by the number of decoys. The recall (sensitivity) values at score threshold <0 show that 74 percent of the actives were selected in all three parallels; however, the precision was low, reflecting that a substantial number of decoys had also been selected. At score threshold <-10, the recall decreased as lower numbers of actives were selected; however, the precision had increased as the reduction in the number of decoys was higher than the reduction in number of actives. This is also reflected by the increased enrichment of the actives at score threshold <-10 compared with score threshold <0. The MCC values did not differ much between the two score thresholds and ranged between 0.27 and 0.41.

The test set was also docked into the binding pocket detected in the outward-facing homology model of SERT using a regular rigid receptor–flexible ligand approach (results not shown). Using this method, only 3 of 19 negatively scored actives and 13 of 190 negatively scored decoys docked in the binding pocket and interacted with D98. However, the majority of actives and decoys were docked outside of the binding pocket, which indicates that the binding pocket in the outward-facing model was too small to accommodate the compounds. This result is in agreement with the results from docking of the compounds belonging to the five SERT inhibitor classes, which showed that the majority of the inhibitors preferred a binding pocket where the distance between the aromatic amino acids of the extracellular gate was increased as compared to in the binding pocket detected in the outward-facing SERT homology model (Fig. 4).

Table 1
Calculated RMSD (Å) values between all pairs of the four generated pharmacophore models (SERT binding pocket conformations 18, 23, 24 and 32).

	Conformation 18	Conformation 23	Conformation 24
Conformation 23	0.95		
Conformation 24	1.05	1.18	
Conformation 32	0.98	1.03	1.14

Table 2
Distances (Å) between the different pharmacophore features in the general pharmacophore model. PI, positive ionisable feature; AR, aromatic feature; HYD, hydrophobic feature; HBA, hydrogen bond acceptor feature.

	AR1	AR2	AR3	AR4	PI	HYD1	HYD2
AR2	0.02						
AR3	4.85	4.83					
AR4	4.88	4.88	0.83				
PI	3.51	3.57	5.54	5.37			
HYD1	0.58	0.58	5.15	5.15	4.05		
HYD2	5.46	5.46	1.01	0.62	5.96	5.74	
HBA	3.79	3.77	2.91	2.46	3.10	4.24	3.02

4. Discussion

Proteins are not rigid structures and should ideally be flexible during docking. However, due to the high number of degrees of freedom that must be taken into account to keep proteins flexible during docking, semi-flexible docking protocols, where the protein is rigid and the ligands flexible, have until recently been most commonly used. Another widely adopted docking strategy is to represent receptor flexibility using an ensemble of rigid snapshots [38], however, the computational complexity of the procedure grows quickly with the numbers of conformers considered. An overview of the new flexible docking protocol used in this study is shown in Fig. 1. The protocol begins with the detection of the ligand binding pocket using ICM PocketFinder [18], followed by biased probability Monte Carlo (BPMC) [19] side chain sampling of the amino acids detected in the binding pocket. The side chain sampling results in the generation of multiple binding pocket conformations, into which the ligands are docked simultaneously

Table 3
Performance indicators of the SERT flexible docking system at two threshold levels (scoring values <0 and <-10) obtained through docking and visual inspection of the evaluation compounds. EF, enrichment factor, MCC, Matthews correlation coefficient.

Score threshold	parallel #	%[a]	EF	MCC	accuracy	precision	recall
<0	1	56	3.02	0.36	0.80	0.27	0.74
	2	57	3.21	0.38	0.81	0.29	0.74
	3	64	2.70	0.33	0.77	0.25	0.74
<-10	1	18.6	4.58	0.41	0.89	0.42	0.53
	2	18.7	3.88	0.27	0.89	0.35	0.32
	3	17.7	4.89	0.38	0.90	0.44	0.42

[a] Percent of compounds with scores better than 0 and −10, respectively.

using the efficient 4D docking protocol described by Bottegoni and co-workers [20].

During the 4D flexible docking into the outward-facing homology model, all 47 binding site conformations with favourable energy generated by side chain sampling were included. This was done to obtain the highest degree of flexibility during docking and to avoid the possible bias that would follow if only selected SERT binding site conformations were used (for instance, the conformations with the lowest energies). Including this many protein conformations may, however, be risky as several studies indicate that using a reduced number of protein conformations result in optimal docking performance [39–44]. In these studies though, crystal structures of soluble proteins were used for docking, while the ligands in our study were docked into a theoretical model of SERT constructed based on a homologous transporter, LeuT [5]. The uncertainty concerning the conformation of the binding site is thus much greater in our SERT homology model than in crystal structures. The diverse structures of the compounds known to interact with SERT, each of which most likely bind to different SERT conformations [14,29], also support the use of several SERT binding pocket conformations.

The major difference between the outward-facing homology model constructed based on the LeuT-tryptophan crystal structure [5] and the occluded SERT homology model based on the X-ray structure of LeuT with leucine bound in the substrate binding site (PDB id 2A65) [28], or based on the LeuT-imipramine crystal structure (PDB id 2Q72) [6], was the localisation of the aromatic amino acids of the extracellular gating residues Y176 (TM3) and F335 (TM8), which in the outward-facing structure were located further apart than in the occluded homology models (4.4 Å vs. 2.3 Å, respectively) (Fig. 4). The difference in distance was the result of large-scale helical movements observed in the L-tryptophan-bound LeuT structure [5]. In the outward-facing model, the putative substrate and vestibular binding sites in the occluded conformation of SERT are detected as one pocket by ICM PocketFinder (Fig. 2). However, the outward-facing SERT homology model was generated based on the x-ray structure of LeuT cocrystallised with the inhibitor L-tryptophan, which is much smaller than known SERT inhibitors. Thus, the distance between these aromatic side chains was still narrow in the outward-facing SERT conformation and the gate in this structure can be considered to be just partly open. Hence, in order to generate binding site conformations where the extracellular gate was more open, side chain sampling was necessary. Our results show that the distance between Y176 and F335 in the four most populated SERT binding site conformations (containing 28 of 54 ligands that could be docked) ranged from approximately 8.7–12.6 Å (Fig. 4). All docked inhibitors preferred a binding pocket conformation where the distance between the side chains of Y176 and F335 was more than 5.3 Å (supplementary data).

Based on our docking results we here propose that inhibitors may bind in an area corresponding to the putative substrate binding site and the vestibular site seen in the LeuT crystal structures. A clear trend in how the known inhibitors bind into the different SERT binding pocket conformations of the outward-facing model (Fig. 5 and supplementary data) was observed. The majority of the compounds have an aromatic ring moiety (that very often is halogenated) protruding out of the putative substrate binding site towards Y176 (TM3) and F335 (TM8) and into the extracellular vestibule, and thus our results may suggest that inhibitors interfere with transport in SERT by preventing closure of the extracellular gate. This inhibition mechanism has recently also been proposed by another group [45]. The four generated structure–docking-based pharmacophore models and the general pharmacophore model (Fig. 6) explain the binding mode of different types of known SERT inhibitors used in this study. The minor differences in the spatial rearrangement of features can be caused by the ambiguous averaging of pharmacophore points (or vectors in the case of aromatic ring and hydrogen bond acceptor feature) and the topological variety of docked ligands to a given conformation. In our homology model, amino acid F335 is not found in the unwound region of TM6 (Fig. 3). However, in a recently published study amino acids 334–337 were suggested to be in an unwound region of SERT based on aqueous accessibility data [46]. The notion that the HBA feature of our pharmacophore models points in the direction of F335 (TM6) indicates that the exposure of main chain atoms and helix dipoles, factors known to play key roles in the binding of leucine and sodium ions in LeuT, also may be important in the binding of inhibitors in SERT (Fig. 6). The localisation of the HBA feature in the direction of F335 could also be explained by the creation of weak C–H···O hydrogen bonds between the ligands and the side chain hydrogen atoms of F335 [47–49]. To our knowledge, the pharmacophore models generated in this study are the first comprehensive models that incorporate ligands from structurally diverse groups and are based on several SERT conformations. Previously published SERT pharmacophore models focused only on limited classes of ligands [50,51]. The methodology of general pharmacophore model generation is quite similar to the strategy of dynamic receptor-based pharmacophore model developed by Deng et al. [52], the major difference being that structurally diverse ligands were used here whereas only one ligand was studied by Deng et al. [52].

The crystal structures of LeuT cocrystallised with inhibitors belonging to the SSRI and TCA classes of antidepressant drugs has led to the suggestion that these inhibitors bind in a corresponding vestibular binding site in SERT [6,8,9,53]. There are, however, some important differences between LeuT and SERT regarding the binding of TCAs and SSRIs. Contrary to their affinities for SERT, the affinities of the cocrystallised TCAs and SSRIs for LeuT are low [6,8,9]. Moreover, the amino acids anchoring the cocrystallised antidepressants in LeuT are not totally conserved between LeuT and SERT, and one important amino acid, LeuT D401, in fact corresponds to a lysine (K490) in SERT [3]. Multiple studies on SERT that have combined homology modelling and docking approaches with site-directed mutagenesis methods indicate that inhibitors interact with SERT in the centrally located putative substrate binding site. For instance, mutations of Y95, D98 (TM1), I172, Y176 (TM3), F335, F341 (TM6) and S438 (TM8), all of which are located in the putative substrate binding site of SERT, have been shown to affect binding of multiple inhibitors, including the SSRIs fluoxetine, citalopram, sertraline, fluvoxamine, and venlafaxine and the TCAs clomipramine, amitriptyline, desipramine, and imipramine [12,13,30–32,45,54–57]. Studies have suggested that the amine moiety of TCAs forms a salt bridge with D98 (TM1), whereas the 3-position of the compounds may point towards A173/T439 and the 7-position towards F335 (TM6) [45]. The orientations of the TCAs obtained through docking into the outward-facing homology model in the present study are in general agreement with the abovementioned results, with the exception of clomipramine, whose 3-chloro substituent was pointing in the direction of F335 (TM6), not A173/T439 (Supporting information table S2). Studies have also suggested that the fluorophenyl moiety of (*S*)-citalopram is oriented towards I172, A173 and N177 (TM3) while the cyanophtalane moiety of the ligand possibly is oriented towards V343 (TM6) [11]. Our results support the localisation of the fluorophenyl moiety of this ligand, however, not the localisation of the cyanophtalane moiety, which in the present study was pointing towards EL4 (Supporting information table S1).

In order to see how the 58 known SERT inhibitors may be oriented in the vestibular binding region, the inhibitors were docked into a SERT homology model based on the LeuT-imipramine

crystal structure (PDB id 2Q72). Docking of the 58 known SERT inhibitors into the vestibular binding site of this homology model, however, showed that the inhibitors did not occupy a region in SERT similar to that of TCA and SSRI in LeuT, and also showed that the orientations of the ligands were significantly more varied than observed in the outward-facing model. The results hence suggest that the vestibular binding region corresponding to the vestibular binding site in LeuT is not the primary binding site for these inhibitors in SERT. However, though our results indicate that the inhibitors are competitive inhibitors that interact in the central putative substrate binding site (and protrude out in the vestibular region), we cannot rule out that the inhibitors, or at least some of the inhibitors, may interact with SERT in the vestibular site and not merely pass through this region *en route* to the central substrate binding site. EL4 plays an important role in binding of the cocrystallised ligands in the LeuT crystal structures, however, superimposition of the LeuT-TCA/SSRI crystal structures show that orientation of EL4 varies [6,8,9], which is also supported by data from SERT [58]. Loop sampling may hence be necessary to dock inhibitors into the vestibular region of SERT. In the present study, however, only the side chains of the amino acids were sampled.

The flexible docking protocol described in this paper is a simple and time-efficient way to generate multiple binding pocket conformations that can be used for dock a large number of compounds in one docking run. The present docking protocol differs from the often-used induced-fit docking (IFD) method available from Schrödinger [59]. In IFD, an initial regular flexible ligand/rigid protein docking is performed to generate an ensemble of 20 ligand poses, followed by molecular dynamics force-field based sampling of the amino acids that have at least one atom within 5 Å of any of the 20 ligand poses from the previous step. During this sampling, both the backbone and side chains are free to move. The ligand is then redocked and scored. Thus, in IFD, the final docking result is highly dependent on the orientation of the ligand docked into the rigid protein. In the present flexible docking protocol, multiple binding site conformations were generated prior to docking and hence independently of the orientation of a docked ligand. In the outward-facing SERT model, the extracellular gate (Y176 and F335) was not fully opened and the lower region of the pocket (the putative substrate binding site) was partly separated from the more extracellular parts of the pocket, restricting the docking of larger competitive inhibitors. During the BPMC side chain sampling, however, several binding pocket conformations with increased distance between Y176 and F335 were generated and 54 of the 58 large and structurally diverse inhibitors were able to dock with their protonated amine group interacting with D98.

The 4D docking method, the last step in the present docking protocol, has previously been validated and shown to reproduce the ligand binding geometry in 77.3 percent of the tested x-ray crystallography structures [20]. In this study, the flexible docking protocol and the binding pocket conformations were evaluated by docking of a test set containing highly potent SERT inhibitors and decoys in a 1:10 ratio. Docking of the test set into the outward-facing SERT model using a regular rigid receptor–flexible ligand approach showed that only three of 19 actives and 13 of 190 decoys docked into the binding pocket and interacted with D98. The docking results, however, greatly improved when the test set was docked using the flexible docking protocol. Using the flexible docking approach, around 80 percent of the actives and decoys were correctly predicted at a threshold <0, and around 90 percent at a threshold <-10. The docked complexes with didesmethyl-(*S*)-citalopram, 403U76, imipramine, (*R*)-mazindol and RTI-311 were refined in several steps resulting in 25 refined binding pocket conformations. Re-docking of these five inhibitors into the 25 refined models improved the scoring in some of the refined models, but not in others (results not shown). The test set was also docked into 25 refined binding pocket conformations. At a score threshold of <-10, the obtained enrichment factors from docking into the refined structures ranged from 1.00 to 4.00, indicating that the refinements did not improve the docking results (Table 3).

Table 4
Ligand RMSD (heavy atoms) between the docked and the crystallised ligands. The PDB codes of the target structures and of the complex containing the ligands are given. COX-2: cyclooxygenase-2, ER: oestrogen receptor, LeuT: the *Aquifex aeolicus* leucine transporter.

Protein	Target	Ligand	Ligand RMSD (Å)	
			Regular docking	Flexible docking
LeuT	2A65	3F3C	2.1	2.1
	3F3C	2A65	3.8	3.9
COX-2	1CX2	3PGH	14.8	1.5
	3PGH	1CX2	13.8	1.0
ER	3ERT	1ERR	2.6	2.6
	1ERR	3ERT	7.5	7.6

A limitation with our test set may be that it only contained strong SERT binders, whereas in virtual screening studies only few ligands may be high-affinity binders. However, the docking of the 58 known SERT inhibitors and the evaluation test set ligands indicated that the present docking protocol worked well for docking structurally diverse compounds into the flexible 5-HT transporter. The majority of the known inhibitors docked and interacted with D98, and the predictability of the model improved greatly when the flexible ligand docking approach was used.

The results from the cross-docking studies (Table 4) also indicated that the flexible docking protocol in some cases may improve docking in crystal structures as compared to regular semi-flexible docking protocols. Great improvements in the docking results were seen for COX-2, where the ligands did not dock in the binding site using a rigid receptor but docked well when the flexible protocol was used (RMSD $<$ 1.5 Å; Table 4). The RMSD values obtained from cross-docking in COX-2 were quite similar to those obtained in a similar cross-docking study using IFD [59]. Cross-docking of the 1ERR ligand into the 3ERT oestrogen receptor yielded an RMSD of 2.6 Å both using a regular docking approach and the flexible docking approach (Table 4). Docking of the 3ERT ligand into the 1ERR receptor showed that the docked ligand could occupy the same area in the binding pocket as in the crystal structure, however, that it preferred a flipped orientation as compared with the crystallised ligand both in the rigid and flexible docking approaches. Due to the flip, the RMSD values obtained were quite large (Table 4). The corresponding RMSD values obtained using IFD were 1.4 and 1.0 Å [59]. However, the binding pocket in the oestrogen receptor was very narrow and in the IFD some of the amino acids in the binding site had been mutated to alanine prior to docking [59], which was not done in our cross-docking study. For LeuT, two crystal structures of the transporter in an occluded conformation were selected due to the lack of multiple outward-facing LeuT 3D structures. The cross-docking showed that the results from the rigid docking did not improve when a flexible docking protocol was used (Table 4). This is not surprising, however, as the RMSD between the amino acids in the substrate binding pocket of 2A65 and 3F3C was only 0.3 Å.

5. Conclusions

In this study, an outward-facing SERT homology model and an occluded SERT homology model using the crystal structures of LeuT cocrystallised with L-tryptophan and imipramine as templates [5,6]. The models were used for docking of 58 known inhibitors

using a new flexible docking protocol. Based on the docking results we propose that the docking favour the outward-facing model. Our docking results also indicated that the majority of the inhibitors preferred a binding pocket where the distance between the aromatic side chains of the extracellular gate (Y176, F335) was greater than in the initial outward-facing SERT homology model. The inhibitors interacted with amino acids located both in the putative substrate binding pocket and in the vestibular region, and the binding mode was illustrated by a general pharmacophore model. Docking a test set containing 19 actives and 190 decoys into the ensemble of 47 binding pocket conformations of the outward-facing model also showed that the ensemble was able to discriminate the majority of the active from inactive compounds. These results could not be obtained using a regular rigid receptor–flexible ligand approach. The new flexible docking protocol may thus give insights into ligand binding that otherwise would not have been detected. Also, the overall sequence identity between SERT and the template LeuT is only 21%. The present results thus indicate that the flexible docking protocol may be a valuable approach in structure-based virtual screening experiments, even when homology models of flexible proteins with low identity with the template is used for screening.

Acknowledgements

This work was supported by a grant from the Nevronor program of the Research Council of Norway (project 176956/V40), the Polish-Norwegian Research Fund (grant PNRF-103-AI-1/07) and the University of Tromsø, Norway. The work was also supported by grants from National Institutes of Health USA (grant numbers R01 GM071872, U01 GM094612, U54 GM094618, and RC2 LM 010994)

Appendix. Supplementary data

Supplementary data associated with this article can be found, in the online version, at doi:10.1016/j.ejmech.2011.09.056.

References

[1] D.T. Wong, K.W. Perry, F.P. Bymaster, Case history: the discovery of fluoxetine hydrochloride (Prozac), Nat. Rev. Drug Discov. 4 (2005) 764–774.
[2] M.H. Saier Jr., A functional-phylogenetic classification system for transmembrane solute transporters, Microbiol. Mol. Biol. Rev. 64 (2000) 354–411.
[3] T. Beuming, L. Shi, J.A. Javitch, H. Weinstein, A comprehensive structure-based alignment of prokaryotic and eukaryotic neurotransmitter/Na+ symporters (NSS) aids in the use of the LeuT structure to probe NSS structure and function, Mol. Pharmacol. 70 (2006) 1630–1642.
[4] M. Tatsumi, K. Groshan, R.D. Blakely, E. Richelson, Pharmacological profile of antidepressants and related compounds at human monoamine transporters, Eur. J. Pharmacol. 340 (1997) 249–258.
[5] S.K. Singh, C.L. Piscitelli, A. Yamashita, E. Gouaux, A competitive inhibitor traps LeuT in an open-to-out conformation, Science 322 (2008) 1655–1661.
[6] S.K. Singh, A. Yamashita, E. Gouaux, Antidepressant binding site in a bacterial homologue of neurotransmitter transporters, Nature 448 (2007) 952–956.
[7] A. Yamashita, S.K. Singh, T. Kawate, Y. Jin, E. Gouaux, Crystal structure of a bacterial homologue of Na^+/Cl^-dependent neurotransmitter transporters, Nature 437 (2005) 215–223.
[8] Z. Zhou, J. Zhen, N.K. Karpowich, R.M. Goetz, C.J. Law, M.E. Reith, D.N. Wang, LeuT-desipramine structure reveals how antidepressants block neurotransmitter reuptake, Science 317 (2007) 1390–1393.
[9] Z. Zhou, J. Zhen, N.K. Karpowich, C.J. Law, M.E. Reith, D.N. Wang, Antidepressant specificity of serotonin transporter suggested by three LeuT-SSRI structures, Nat. Struct. Mol. Biol. 16 (2009) 652–657.
[10] E.M. Adkins, E.L. Barker, R.D. Blakely, Interactions of tryptamine derivatives with serotonin transporter species variants implicate transmembrane domain I in substrate recognition, Mol. Pharmacol. 59 (2001) 514–523.
[11] J. Andersen, L. Olsen, K.B. Hansen, O. Taboureau, F.S. Jorgensen, A.M. Jorgensen, B. Bang-Andersen, J. Egebjerg, K. Stromgaard, A.S. Kristensen, Mutational mapping and modeling of the binding site for (S)-citalopram in the human serotonin transporter, J. Biol. Chem. 285 (2010) 2051–2063.
[12] L.K. Henry, J.R. Field, E.M. Adkins, M.L. Parnas, R.A. Vaughan, M.F. Zou, A.H. Newman, R.D. Blakely, Tyr-95 and Ile-172 in transmembrane segments 1 and 3 of human serotonin transporters interact to establish high affinity recognition of antidepressants, J. Biol. Chem. 281 (2006) 2012–2023.
[13] C.C. Walline, D.E. Nichols, F.I. Carroll, E.L. Barker, Comparative molecular field analysis using selectivity fields reveals residues in the third transmembrane helix of the serotonin transporter associated with substrate and antagonist recognition, J. Pharmacol. Exp. Ther. 325 (2008) 791–800.
[14] S. Tavoulari, L.R. Forrest, G. Rudnick, Fluoxetine (Prozac) binding to serotonin transporter is modulated by chloride and conformational changes, J. Neurosci. 29 (2009) 9635–9643.
[15] Y.W. Zhang, G. Rudnick, The cytoplasmic substrate permeation pathway of serotonin transporter, J. Biol. Chem. 281 (2006) 36213–36220.
[16] M.T. Jacobs, Y.W. Zhang, S.D. Campbell, G. Rudnick, Ibogaine, a noncompetitive inhibitor of serotonin transport, acts by stabilizing the cytoplasm-facing state of the transporter, J. Biol. Chem. 282 (2007) 29441–29447.
[17] O. Jardetzky, Simple allosteric model for membrane pumps, Nature 211 (1966) 969–970.
[18] J. An, M. Totrov, R. Abagyan, Pocketome via comprehensive identification and classification of ligand binding envelopes, Mol. Cell Proteomics 4 (2005) 752–761.
[19] R. Abagyan, M. Totrov, Biased probability Monte Carlo conformational searches and electrostatic calculations for peptides and proteins, J. Mol. Biol. 235 (1994) 983–1002.
[20] G. Bottegoni, I. Kufareva, M. Totrov, R. Abagyan, Four-dimensional docking: a fast and accurate account of discrete receptor flexibility in ligand docking, J. Med. Chem. 52 (2009) 397–406.
[21] R. Apweiler, A. Bairoch, C.H. Wu, W.C. Barker, B. Boeckmann, S. Ferro, E. Gasteiger, H. Huang, R. Lopez, M. Magrane, M.J. Martin, D.A. Natale, C. O'Donovan, N. Redaschi, L.S. Yeh, UniProt: the universal protein knowledgebase, Nucleic Acids Res. 32 (2004) D115–D119.
[22] R. Abagyan, M. Totrov, D. Kuznetsov, ICM – a new method for protein modeling and design: applications to docking and structure prediction from the distorted native conformation, J. Computational Chem. 15 (1994) 488–506.
[23] R. Abagyan, I. Kufareva, The flexible pocketome engine for structural chemogenomics, Methods Mol. Biol. 575 (2009) 249–279.
[24] M. Schapira, R. Abagyan, M. Totrov, Nuclear hormone receptor targeted virtual screening, J. Med. Chem. 46 (2003) 3045–3059.
[25] Discovery Studio, in: Accelrys Inc., San Diego, CA, USA.
[26] B.W. Matthews, Comparison of the predicted and observed secondary structure of T4 phage lysozyme, Biochim. Biophys. Acta 405 (1975) 442–451.
[27] D.A. Pearlman, P.S. Charifson, Improved scoring of ligand-protein interactions using OWFEG free energy grids, J. Med. Chem. 44 (2001) 502–511.
[28] A.W. Ravna, I. Sylte, S.G. Dahl, Structure and localisation of drug binding sites on neurotransmitter transporters, J. Mol. Model. 15 (2009) 1155–1164.
[29] R.B. Rothman, M.H. Baumann, B.E. Blough, A.E. Jacobson, K.C. Rice, J.S. Partilla, Evidence for noncompetitive modulation of substrate-induced serotonin release, Synapse, 64 862–869.
[30] J. Andersen, O. Taboureau, K.B. Hansen, L. Olsen, J. Egebjerg, K. Stromgaard, A.S. Kristensen, Location of the antidepressant binding site in the serotonin transporter: importance of Ser-438 in recognition of citalopram and tricyclic antidepressants, J. Biol. Chem. 284 (2009) 10276–10284.
[31] E.L. Barker, K.R. Moore, F. Rakhshan, R.D. Blakely, Transmembrane domain I contributes to the permeation pathway for serotonin and ions in the serotonin transporter, J. Neurosci. 19 (1999) 4705–4717.
[32] L. Celik, S. Sinning, K. Severinsen, C.G. Hansen, M.S. Moller, M. Bols, O. Wiborg, B. Schiott, Binding of serotonin to the human serotonin transporter. Molecular modeling and experimental validation, J. Am. Chem. Soc. 130 (2008) 3853–3865.
[33] K.W. Kaufmann, E.S. Dawson, L.K. Henry, J.R. Field, R.D. Blakely, J. Meiler, Structural determinants of species-selective substrate recognition in human and *Drosophila* serotonin transporters revealed through computational docking studies, Proteins 74 (2009) 630–642.
[34] V. Katritch, I. Kufareva, R. Abagyan, Structure based prediction of subtype-selectivity for adenosine receptor antagonists, Neuropharmacology 60 (2011) 108–115.
[35] V. Katritch, K.A. Reynolds, V. Cherezov, M.A. Hanson, C.B. Roth, M. Yeager, R. Abagyan, Analysis of full and partial agonists binding to beta2-adrenergic receptor suggests a role of transmembrane helix V in agonist-specific conformational changes, J. Mol. Recognit 22 (2009) 307–318.
[36] V. Katritch, M. Rueda, P.C. Lam, M. Yeager, R. Abagyan, GPCR 3D homology models for ligand screening: lessons learned from blind predictions of adenosine A2a receptor complex, Proteins 78 (2010) 197–211.
[37] I. Kufareva, M. Rueda, V. Katritch, R.C. Stevens, R. Abagyan, Status of GPCR modeling and docking as reflected by community-wide GPCR dock 2010 assessment, Structure 19 (2011) 1108–1126.
[38] M. Totrov, R. Abagyan, Flexible ligand docking to multiple receptor conformations: a practical alternative, Curr. Opin. Struct. Biol. 18 (2008) 178–184.
[39] X. Barril, S.D. Morley, Unveiling the full potential of flexible receptor docking using multiple crystallographic structures, J. Med. Chem. 48 (2005) 4432–4443.
[40] M. Rueda, G. Bottegoni, R. Abagyan, Recipes for the selection of experimental protein conformations for virtual screening, J Chem Inf Model, 50 186–193.
[41] M.P. Thomas, C. McInnes, P.M. Fischer, Protein structures in virtual screening: a case study with CDK2, J. Med. Chem. 49 (2006) 92–104.

[42] M.L. Verdonk, P.N. Mortenson, R.J. Hall, M.J. Hartshorn, C.W. Murray, Protein–ligand docking against non-native protein conformers, J. Chem. Inf. Model. 48 (2008) 2214–2225.
[43] S. Yoon, W.J. Welsh, Identification of a minimal subset of receptor conformations for improved multiple conformation docking and two-step scoring, J. Chem. Inf. Comput. Sci. 44 (2004) 88–96.
[44] S. Rao, P.C. Sanschagrin, J.R. Greenwood, M.P. Repasky, W. Sherman, R. Farid, Improving database enrichment through ensemble docking, J. Comput. Aided Mol. Des 22 (2008) 621–627.
[45] S. Sinning, M. Musgaard, M. Jensen, K. Severinsen, L. Celik, H. Koldso, T. Meyer, M. Bols, H.H. Jensen, B. Schiott, O. Wiborg, Binding and orientation of tricyclic antidepressants within the central substrate site of the human serotonin transporter, J. Biol. Chem. 285 (2010) 8363–8374.
[46] J.R. Field, L.K. Henry, R.D. Blakely, Transmembrane domain 6 of the human serotonin transporter contributes to an aqueously accessible binding pocket for serotonin and the psychostimulant 3,4-methylene dioxymethamphetamine, J. Biol. Chem., 285 11270–11280.
[47] A.C. Pierce, K.L. Sandretto, G.W. Bemis, Kinase inhibitors and the case for CH.O hydrogen bonds in protein-ligand binding, Proteins 49 (2002) 567–576.
[48] A.C. Pierce, E. ter Haar, H.M. Binch, D.P. Kay, S.R. Patel, P. Li, CH.O and CH.N hydrogen bonds in ligand design: a novel quinazolin-4-ylthiazol-2-ylamine protein kinase inhibitor, J. Med. Chem. 48 (2005) 1278–1281.
[49] C. Bissantz, B. Kuhn, M. Stahl, A medicinal chemist's guide to molecular interactions, J Med Chem, 53 5061–5084.
[50] I.J. Macdougall, R. Griffith, Pharmacophore design and database searching for selective monoamine neurotransmitter transporter ligands, J. Mol. Graph Model. 26 (2008) 1113–1124.
[51] L. Orus, S. Perez-Silanes, A.M. Oficialdegui, J. Martinez-Esparza, J.C. Del Castillo, M. Mourelle, T. Langer, S. Guccione, G. Donzella, E.M. Krovat, K. Poptodorov, B. Lasheras, S. Ballaz, I. Hervias, R. Tordera, J. Del Rio, A. Monge, Synthesis and molecular modeling of new 1-aryl-3-[4-arylpiperazin-1-yl]-1-propane derivatives with high affinity at the serotonin transporter and at 5-HT(1A) receptors, J. Med. Chem. 45 (2002) 4128–4139.
[52] J. Deng, K.W. Lee, T. Sanchez, M. Cui, N. Neamati, J.M. Briggs, Dynamic receptor-based pharmacophore model development and its application in designing novel HIV-1 integrase inhibitors, J. Med. Chem. 48 (2005) 1496–1505.
[53] S. Sarker, R. Weissensteiner, I. Steiner, H.H. Sitte, G.F. Ecker, M. Freissmuth, S. Sucic, The high-affinity binding site for tricyclic antidepressants resides in the outer vestibule of the serotonin transporter, Mol. Pharmacol..
[54] J.G. Chen, A. Sachpatzidis, G. Rudnick, The third transmembrane domain of the serotonin transporter contains residues associated with substrate and cocaine binding, J. Biol. Chem. 272 (1997) 28321–28327.
[55] B.J. Thompson, T. Jessen, L.K. Henry, J.R. Field, K.L. Gamble, P.J. Gresch, A.M. Carneiro, R.E. Horton, P.J. Chisnell, Y. Belova, D.G. McMahon, L.C. Daws, R.D. Blakely, Transgenic elimination of high-affinity antidepressant and cocaine sensitivity in the presynaptic serotonin transporter, Proc. Natl. Acad. Sci. United State. America 108 (2011) 3785–3790.
[56] E.L. Barker, M.A. Perlman, E.M. Adkins, W.J. Houlihan, Z.B. Pristupa, H.B. Niznik, R.D. Blakely, High affinity recognition of serotonin transporter antagonists defined by species-scanning mutagenesis. An aromatic residue in transmembrane domain I dictates species-selective recognition of citalopram and mazindol, J. Biol. Chem. 273 (1998) 19459–19468.
[57] P. Plenge, U. Gether, S.G. Rasmussen, Allosteric effects of R- and S-citalopram on the human 5-HT transporter: evidence for distinct high- and low-affinity binding sites, Eur. J. Pharmacol. 567 (2007) 1–9.
[58] S.M. Mitchell, E. Lee, M.L. Garcia, M.M. Stephan, Structure and function of extracellular loop 4 of the serotonin transporter as revealed by cysteine-scanning mutagenesis, J. Biol. Chem. 279 (2004) 24089–24099.
[59] W. Sherman, T. Day, M.P. Jacobson, R.A. Friesner, R. Farid, Novel procedure for modeling ligand/receptor induced fit effects, J. Med. Chem. 49 (2006) 534–553.